0026-895X/95/030559-09$3.00/0

MOLECULAR PHARMACOLOGY, 48:559–567 (1995).

A Single Amino Acid Change in the Mouse Peroxisome Proliferator-Activated Receptor α Alters Transcriptional Responses to Peroxisome Proliferators

MEI-HUI HSU, COLIN N. A. PALMER, KEITH J. GRIFFIN, and ERIC F. JOHNSON

Department of Molecular and Experimental Medicine, The Scripps Research Institute, La Jolla, California 92037

Received April 20, 1994; Accepted June 19, 1995

SUMMARY

The mouse peroxisome proliferator-activated receptor α (mPPARα) can activate transcription from the *CYP4A6* promoter in transient cotransfection experiments in the absence (intrinsic transactivation) or presence of added peroxisome proliferator. However, mPPARα-G, in which glycine is substituted for Glu^{282}, exhibits very low intrinsic transactivation and responds fully to added peroxisome proliferators. The two receptors, when expressed in COS-1 cells, are nuclear in localization, are expressed at similar levels, have similar stability, and bind DNA *in vitro* with similar efficiency. The phenotypic difference in intrinsic transactivation is not altered by overexpression of the human retinoid X receptor α. The mPPARα-G mutant receptor displays a higher EC_{50} for pirinixic acid and for 5,8,11,14-eicosatetraynoic acid than the wild-type PPARα. This difference in the apparent EC_{50} value is independent of the cell lines used and indicates that the Glu^{282} to glycine substitution alters the response of mPPARα to peroxisome proliferators. The EC_{50} values obtained for each receptor with the *CYP4A6* reporter construct are lower than those for a reporter derived from the acyl-CoA oxidase gene. In general, an inverse relation is evident between the apparent EC_{50} values and the extent of intrinsic transactivation observed. The difference in intrinsic transactivation may reflect the presence of an endogenous activator at a concentration that is not sufficient to activate the mPPARα-G but that is sufficient to effect the intrinsic transactivation seen for the wild-type mPPARα.

The mPPARα is a member of the steroid receptor gene superfamily that was first cloned from mouse liver (1) and subsequently has been identified in several other species, including human (2), *Xenopus* (3), and rat (4). PPARα, which is one of at least three subtypes of PPARs, can be activated by a diverse group of peroxisome proliferators that includes hypolipidemic drugs such as clofibrate and plasticizers such as mono(2-ethylhexyl)phthalate (1, 5). Peroxisome proliferators elicit pleiotropic responses in rodents, which include liver hypertrophy and hyperplasia, accompanied by an increase in the number of peroxisomes in hepatic parenchymal cells. Long term exposure to peroxisome proliferators produces liver tumors in rodents but not in primates (6–8). In addition to increasing the number of peroxisomes, peroxisome proliferators induce the enzymes that catalyze peroxisomal (9, 10) and microsomal fatty acid oxidation (10–12). Recently, fatty acids have been shown to activate PPAR (4, 13), and it has been suggested that they could represent endogenous ligands for this receptor (13–16). However, none of the activating compounds have been shown to bind directly to PPARα, and the mechanism by which peroxisome proliferators activate transcription through PPARα is unclear.

PPARα has been shown to regulate the transcription of several peroxisome proliferator-responsive genes, including ACO (17, 18), the enoyl-CoA hydratase/3-hydroxyacyl CoA dehydrogenase (bifunctional enzyme) (19, 20), and the microsomal fatty acid ω-hydroxylases, P-450[1] 4A1 (21) and 4A6 (22). The binding of PPARα to specific response elements mapped in the 5′ flanking region of the genes for these enzymes *in vitro* is facilitated by a second member of the

This work was supported by United States Public Health Service Grant HD04445 (E.F.J.) and Postdoctoral Fellowship 93–96 from the American Heart Association of California (C.N.A.P.). Facilities for computer-assisted analysis and the synthesis of oligonucleotides are supported in part by General Clinical Research Center Grant M01RR00833 and by the Sam and Rose Stein Charitable Foundation, respectively.

[1] Individual P-450s are designated according to a uniform system of nomenclature (41) and the gene designations are preceded by the letters CYP.

ABBREVIATIONS: mPPARα, mouse peroxisome proliferator-activated receptor α; ACO, peroxisomal fatty acyl-CoA oxidase; BSA, bovine serum albumin; DMSO, dimethylsulfoxide; DTT, dithiothreitol; EMSA, electrophoretic mobility-shift analysis; ETYA, 5,8,11,14-eicosatetraynoic acid; GST, glutathione *S*-transferase; IMPB, immunoprecipitation buffer; mPPARα-G, a mutant form of mPPARα; nt, nucleotide; PBS, phosphate-buffered saline; PMSF, phenylmethylsulfonyl fluoride; PPRE, peroxisome proliferator-response element; P-450, a generic term for a cytochrome P-450 mono-oxygenase; RXRα, retinoid X receptor α; SDS-PAGE, sodium dodecyl sulfate-polyacrylamide gel electrophoresis; Wy-14,643, [4-chloro-6-(2,3-xylidino)-2-pyrimidinylthio]acetic acid; DMEM, Dulbecco's modified Eagle's medium.

nuclear receptor family, RXRα (20, 21, 23–27). Cotransfection of RXRα also synergizes reporter gene transactivation (23, 26, 28).

Previous transfection studies in our laboratory (22) demonstrated that transactivation of *CYP4A6* reporter constructs by mPPARα in three different cell lines was independent of the addition of peroxisome proliferators to the cell culture media. For the present study, we call this response intrinsic transactivation. Although this effect had been noted with reporter constructs derived from other genes (2, 3, 27, 29, 30), the intrinsic transactivation is very pronounced with *CYP4A6* reporter constructs and is ~60–80% of the level of transactivation seen with added peroxisome proliferators (22). A very low intrinsic transactivation was seen with a PCR mutant, mPPARα-G, which differs from mPPARα by a single amino acid located at the beginning of the putative ligand binding domain (Glu^{282} to glycine) (1). However, mPPARα-G displays significant peroxisome proliferator-dependent transactivation.

To determine the basis for this difference in intrinsic transactivation, we characterized the mutant PPARα further and compared its properties with those of the wild-type PPARα. Pulse labeling studies with COS-1 cells demonstrate that the mutation does not affect protein stability or the level of expression. Immunocytochemical studies with transfected COS-1 cells and gel mobility shift experiments indicate that the two receptors exhibit the same predominant nuclear localization and a similar ability to bind DNA *in vitro*. Two luciferase reporter constructs were used to compare the dose-response curves of mPPARα and mPPARα-G to examine transcriptional activation in the absence or presence of various peroxisome proliferators. One reporter construct harbors the PPRE of the rat ACO gene in the context of a heterologous promoter, and the other uses the 5′ flanking region of the *CYP4A6* gene with its own promoter.

Materials and Methods

Chemicals. Palmitic acid (hexadecanoic acid) and ETYA were obtained from Sigma Chemical Co. (St. Louis, MO). Wy-14,643 (pirinixic acid) was kindly provided by Dr. C. Pickett (Merck Frosst, Canada). Fetal bovine serum (Lot No. 100–106) was purchased from Gemini (Calabasas, CA), minimum essential medium with Earle's salt was obtained from GIBCO-BRL Life Technologies (Gaithersburg, MD), and DMEM was obtained from BioWhittaker (Walkersville, MD). All other reagents were analytical grade.

Plasmid construction. The pCMV-mPPARα and pCMV-mPPARα-G expression vectors and the reporter plasmids pLuc-4A6–880 and pSV-β-Gal have been described previously (22). The reporter plasmid pLuc-TK-ACO was constructed by linking the -580 to -516 nt segment of the ACO upstream region (17), which contains a PPRE, to the heterologous promoter derived from the *Herpes simplex* thymidine kinase gene (nucleotide 44–200, GenBank M15234). The pRS-hRXRα construct was obtained from Drs. D. J. Manglesdorf and R. Evans, Salk Institute.

Transient transfections. HepG2, RK_{13}, and COS-1 cell lines were obtained from American Type Culture Collection (Rockville, MD), and each was cultured and passaged in T75 flasks (Costar, Cambridge, MA) as suggested by American Type Culture Collection. Before transfection, cells were seeded into Falcon six-well plates (Becton Dickinson, Lincoln Park, NJ). After the density of cells in each well reached 15–20% confluence, the cells were transfected with 5 μg of the reporter construct and 50 ng of the mPPARα expression vector by a modification (26) of the calcium phosphate precipitation method. pSV-β-Gal was also included in the DNA mixture as an internal control to monitor transfection efficiency (2 μg/well for RK_{13} and HepG2 cells and 1 μg/well for COS-1 cells). After 16 hr, the medium was removed, and the test compounds were added into fresh culture medium from a 400× stock solution in DMSO. The final concentration of DMSO in the medium was maintained at 0.25%. The medium was replaced with fresh medium containing test compounds after another 24 hr. The cells were harvested 62 hr after transfection, and luciferase and β-galactosidase activities were determined with clarified whole cell lysates (22). The luciferase activity from each well was expressed relative to the β-galactosidase activity obtained from the same lysate. Triplicate transfections were obtained for each experimental condition. All experiments included transfections with PPARα-G in the presence of 50 μM Wy-14,643 as a basis for normalizing the results obtained with different batches of cells. In each case, the results are reported relative to the results obtained for PPARα-G in the presence of 50 μM Wy-14,643, which was set to an arbitrary value of 100. The mean and standard deviation values were obtained from at least three independent sets of transfection experiments. The dose-response curves were analyzed by nonlinear regression with SlideWrite Plus Version 5 software (Advanced Graphics Software, Carlsbad, CA) to generate the curves shown in the figures and estimates of the EC_{50} values. The equation used for the one-site ligand-binding model was: $y = a0 + [a2(x)/(a1 + x)]$. The equation used for the sigmoidal model was: $y = a0 + a2/\{1 + \exp[-(x - a1)/a3]\}$. For both equations, x is the concentration of the activator compound, y is normalized luciferase activity, $a0$ is intrinsic transactivation, $a1$ is EC_{50}, $a2$ is maximal transactivational response minus intrinsic transactivation, and $a3$ is the width of transition for the sigmoidal response.

For cotransfection with hRXRα, 1 μg/well pRS-hRXRα or the pRS plasmid without insert was included in the DNA transfection mixture. All-*trans*-retinoic acid was added into the medium from a 400× stock solution to a final concentration of 1 μM. The data were normalized as described.

PPARα expression in COS-1 cells and metabolic labeling. COS-1 cells were transfected with 50 ng pCMV-PPARα, pCMV-PPARα-G, or pCMV alone using the DEAE-dextran method (31) in Falcon six-well plates. For immunoblotting, the cells were washed 72 hr after transfection and harvested in PBS (10 mM sodium phosphate, pH 7.4, 150 mM sodium chloride) with a cell scraper. For metabolic labeling, the cells were washed twice with methionine- and cysteine-deficient DMEM (BioWhittaker) and incubated in the deficient medium for 20 min For pulse labeling, 100 μCi/ml Tran^{35}S-label (ICN) was added into the deficient medium, incubated for 1 hr, and chased with changes of complete DMEM for various times (up to 3.5 hr). For general labeling, cells were incubated with 50 μCi/ml Tran ^{35}S-label for 2 hr. Cells were washed with cold PBS and detached with a cell scraper. After centrifugation at 500 × *g* for 10 min, the cell pellet was resuspended in IMPB (50 mM Tris, pH 7.5, containing 1 mM EDTA, 1% Triton X-100, and 0.1% SDS), incubated on ice for 5 min, and then lysed by vigorous passage through a 25-gauge needle (⅝-in length) eight times. The cell lysates were clarified by centrifugation at 15,000 × *g* for 10 min at 4°. The supernatants were removed and stored at −80°. The protein concentration of the supernatant fraction was measured with the use of the Pierce BCA protein assay (Pierce, Rockford, IL).

Antibody production. The mPPARα cDNA was inserted into the pGEX-2T vector as described (26). The GST-mPPARα fusion protein was expressed in *Escherichia coli* DH5α and partially purified using glutathione-conjugated agarose as an affinity column (Sigma). The preparation was eluted from the column with 10 mM reduced glutathione in PBS (containing 2 mM DTT, 1 mM EDTA, 10 mM sodium molybdate, and 10% glycerol). The purity of this affinity purified GST-mPPARα preparation was checked with SDS-PAGE followed by Coomassie blue staining and was estimated to be ~95% pure. Rabbits were injected subcutaneously with 70 μg of fusion protein emulsified with complete Freund's adjuvant (Sigma). After 7 weeks, the

rabbits were given a booster immunization of 50 μg fusion protein emulsified in incomplete Freund's adjuvant, and antisera were collected 2 weeks later.

Immunoblotting. Equal amounts (7 μg) of total protein from transfected COS-1 cell lysates were subjected to SDS-PAGE and transferred electrophoretically to nitrocellulose membranes as described previously (32). The membrane was blocked with PBS containing 3% BSA at 4° overnight before incubation with rabbit anti-mPPARα serum or preimmune serum for 3 hr at room temperature. The sera were diluted 1:200 in PBS containing 3% BSA. ^{125}I-Labeled Protein A (specific activity, >30 μCi/μg; ICN) was used to detect the antigen.

Immunoprecipitation. Equal amounts (15 μg) of total protein from the supernatant fractions of the transfected COS cell lysates prepared in the labeling studies were used for immunoprecipitation as described (33). Briefly, cell lysates were added to 100 μl IMPB containing 0.25% gelatin and 0.1 mM PMSF. Rabbit anti-mPPARα serum (5 μl) was then added and incubated at 4° overnight before the addition of 30 μl of a 1:1 suspension of Protein A/Sepharose (Fast Flow, Sigma). After a 3-hr incubation at 4° on a rotating apparatus, the Protein A/Sepharose was pelleted by brief centrifugation. The Sepharose beads were washed twice with IMPB containing 0.25% gelatin; once with 50 mM Tris, pH 7.5, containing 150 mM NaCl, 1 mM EDTA, and 0.1 mM PMSF; and once with 50 mM Tris, pH 6.8, containing 0.1 mM PMSF. The final washed Sepharose pellets were resuspended in SDS-PAGE loading buffer. The samples were boiled for 5 min and analyzed by SDS-PAGE. The gel was either treated with ENHANCE (Du Pont) as described by the manufacturer and subsequently exposed to Kodak X-ray film at −80° or transferred electrophoretically to a nitrocellulose membrane for immunoblot analysis.

Immunofluorescence. COS-1 cells were cultured in eight-chamber Lab-Tek Permanox Chamber Slides (Nunc, Naperville, IL) and transfected with pCMV-PPARα, pCMV-PPARα-G, or pCMV using either the DEAE-dextran or calcium phosphate transfection methods as described previously (26, 31). The cells were treated with 50 μM Wy-14,643 or DMSO for 48 hr before the media were removed and they were washed twice with cold PBS. The cells were fixed with 4% paraformaldehyde in PBS at 4° overnight. The slides were blocked with PGSN (PBS containing 5 mM glycine, 2% goat serum, 0.1% BSA, and 0.1% NP-40) at 4° overnight and then incubated with rabbit anti-PPARα serum or preimmune serum diluted to 1:50 with PGS (PGSN without NP-40). After an overnight incubation at 4°, the slides were washed four times with PG (PBS containing 5 mM glycine) for 5 min. Goat anti-rabbit IgG conjugated with fluorescein (Calbiochem, La Jolla, CA) diluted with PGSN to 1:30 was added into the chambers and incubated for 2 hr at room temperature. The slides were washed with PG five times and PBS once, mounted with FluorSave (Calbiochem), and viewed with a Zeiss MC100 microscope.

EMSA. COS-1 cells were transfected with 50 ng/well of pCMV-PPARα, pCMV-PPARα-G, or pCMV using the DEAE-dextran method. pSV-β-Gal (1 μg/well) was included in the DNA mixture as an internal control to monitor transfection efficiency. After 24 hr, the cells were treated with 50 μM Wy-14,643 or DMSO for 48 hr before being dislodged into PBS containing 0.2 mM 4-(2-aminoethyl)-benzenesulfonylfluoride hydrochloride (ICN), 2 μg/ml leupeptin, 2 μg/ml aprotinin, and 1 mM DTT. The cell suspension was frozen and thawed three times before sonication for 10 sec. Glycerol was added to the lysates to a final concentration of 10% (v/v), and the lysates were frozen in liquid nitrogen and stored at −70°. The double-stranded oligonucleotide corresponding to the Z element of the *CYP4A6* gene was end labeled with [γ-^{32}P-]ATP as described (26). Cell lysates containing an equal amount of β-galactosidase activity were incubated on ice with 2 μg p(dI-dC) and 2 μg sonicated salmon sperm DNA for 10 min. Radiolabeled Z oligonucleotide (10 fmol) was then added, and the incubation was continued on ice for an additional 10 min. Rabbit anti-mPPARα serum or preimmune serum (0.5 μl) was added to the indicated reactions and incubated on ice for 0.5 hr. Electrophoresis and autoradiography were performed as previously described (26). The gels were also analyzed with a Model SF Molecular Dynamics PhosphoImager (Sunnyvale, CA).

Results

Transactivation with and without added peroxisome proliferators. In the presence of added Wy-14,643 (50 μM), mPPARα and mPPARα-G activate the transcription of the pLuc-4A6–880 reporter construct to similar extents in three cell lines: the rabbit kidney epithelial cell line RK_{13}, the human hepatoma cell line HepG2, and the monkey kidney cell line COS-1 (Fig. 1). In the absence of added Wy-14,643, mPPARα effects significant transactivation of the pLuc-4A6–880 construct in all three cell lines, whereas the transactivation by mPPARα-G is relatively low compared with that observed for the wild-type receptor. This transcriptional activation by mPPARα in the absence of added peroxisome proliferator will be referred to as intrinsic transactivation. In RK_{13} cells, the intrinsic transactivation of pLuc-4A6–880 by mPPARα is approximately 80% of the level of transactivation by mPPARα in the presence of Wy-14,643 compared with 70% in COS-1 cells and 60% in the HepG2 cell line (Fig. 1). When the fetal bovine serum used in the cell culture medium was replaced with charcoal-treated serum to remove small molecules and fatty acids, the level of intrinsic transactivation observed with mPPARα did not change (data not shown), suggesting that these components in serum do not contribute to the difference seen in the level of intrinsic transactivation effected by the two receptors.

The higher intrinsic transactivation seen with the wild-type PPARα compared with mPPARα-G is also evident to a lesser extent with the TK-ACO reporter construct (Fig. 2). The pLuc-TK-ACO construct harbors a PPRE region found in the rat ACO gene (17) that has been placed under the control of a heterologous promoter from the *Herpes simplex* thymidine kinase gene. The level of intrinsic transactivation of pLuc-TK-ACO by the wild-type mPPARα, relative to the level of transactivation seen in the presence of 50 μM Wy-14,643, also varied in the different cell lines, exhibiting the same rank order as pLuc-4A6–880 (RK_{13}, 55%; COS-1, 40%; HepG2, 35%; Fig. 2). In the presence of 50 μM Wy-14,643, mPPARα and mPPARα-G activate the transcription of pLuc-TK-ACO to similar extents in all three cell lines. The wild-type mPPARα exhibits a higher intrinsic transactivation when compared with the mPPARα-G mutant, and the intrinsic transactivation seen with pLuc-TK-ACO construct is lower than that seen with the pLuc-4A6–880 construct in each cell line.

Expression of the two forms of mPPARα. Immunoblotting and pulse-chase labeling of COS-1 cells transfected with expression vectors for either mPPARα or mPPARα-G were used to determine whether there is a difference in protein expression or stability between mPPARα or mPPARα-G. COS-1 cells were chosen because of the greater level of protein expression that results from the higher plasmid copy number in transfected cells. The immunoblot in Fig. 3A demonstrates the specificity of the rabbit antibody toward each mPPARα and indicates that the two forms of mPPARα exhibit similar levels of expression. The pulse-chase experiments (Fig. 3B) indicate that the turnover rates are similar between mPPARα and mPPARα-G for up to 3.5 hr after the

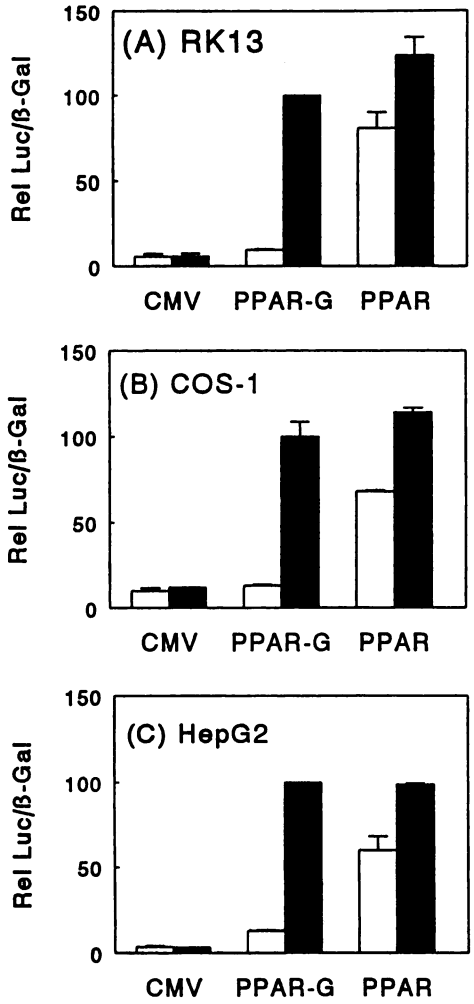

Fig. 1. Transactivation of pLuc-4A6–880 by either mPPARα or mPPARα-G in three different cell lines: A, RK_{13} cells; B, COS-1 cells; C, HepG2 cells. For each well of a six-well plate, cells were transfected with 50 ng pCMV-mPPARα (*PPAR*), pCMV-mPPARα-G (*PPAR-G*), or pCMV (*CMV*) and 5 μg of the pLuc-4A6–880 reporter as described in Materials and Methods. pSV-βGal was also included in the transfection as an internal control. Cells were treated with fresh medium containing DMSO (*open bar*) or 50 μM Wy-14,643 (*filled bar*) daily for 46 hr. Luciferase (*Luc*) activity for each well was normalized with the corresponding β-galactosidase (*β-Gal*) activity determined for the same well. Data are reported relative to the normalized luciferase activity obtained from the cells transfected with mPPARα-G and treated with 50 μM Wy-14,643. This value was arbitrarily set to 100. Mean and standard deviation values for each data point are the average of at least three transfections. For each transfection experiment, triplicate determinations were obtained for each set of experimental conditions.

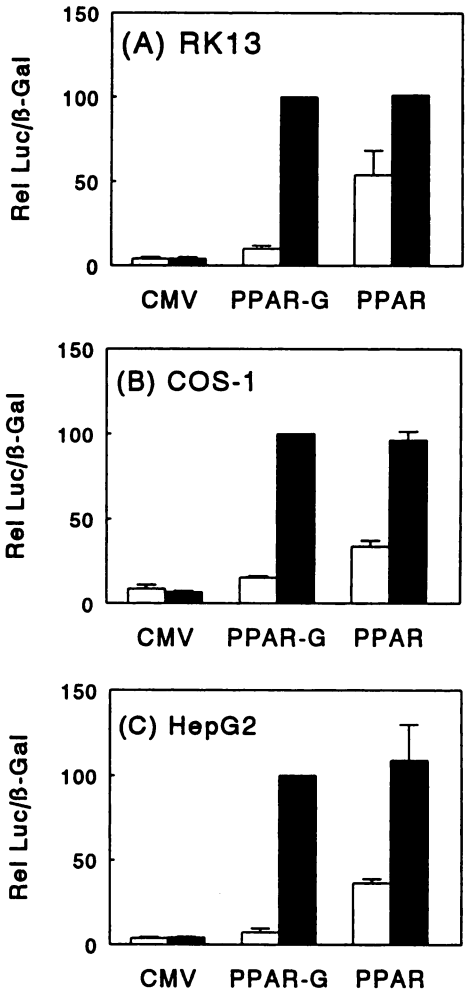

Fig. 2. Transactivation of pLuc-TK-ACO by either mPPARα or mPPARα-G in three different cell lines: A, RK_{13} cells; B, COS-1 cells; C, HepG2 cells. Cells were transfected with pCMV-mPPARα (*PPAR*), pCMV-mPPARα-G (*PPAR-G*), or pCMV (*CMV*) and the pLuc-TK-ACO reporter as described in Fig. 1. DMSO (*open bar*) or 50 μM Wy-14,643 (*filled bar*) was included into fresh medium changed daily as described in Materials and Methods. The data are expressed as described for Fig. 1.

1-hr pulse labeling. These results indicate that the higher intrinsic transactivation for the wild-type mPPARα does not reflect a difference in the level of protein expression or the turnover rate of the two mPPARs.

Subcellular localization of mPPARα and mPPARα-G. A predominately nuclear localization has been reported for xPPARα and xPPARβ in transfected COS-1 cells and *Xenopus laevis* oocytes (34) and for rPPARα in rat brain (35). Therefore, immunofluoroscence studies of COS-1 cells transfected with expression vectors for either mPPARα and mPPARα-G were used to determine whether there is a difference in the subcellular localization after their synthesis. In the absence of added peroxisome proliferator, the mutant mPPARα-G is localized predominately in the nuclei of the transfected COS-1 cells (Fig. 4C), as is seen for the wild-type PPARα (Fig. 4A). Due to the inefficiency of transfection with the calcium phosphate method, only a small percentage of the COS cells expressed the PPARα. Those cells in Fig. 4 (A and C) that did not express the receptor had a diffuse cytosolic background staining similar to either cells transfected with PPARα and treated with preimmune serum (Fig. 4B) or cells transfected with the pCMV vector only (Fig. 4D). This predominately nuclear localization in transfected COS cells was not altered when Wy-14,643 was added to the culture medium (data not shown). Also, the localization did not change when the DEAE-dextran method, which yields a higher transfection efficiency than the calcium phosphate method, was used for the transient expression of either PPARα (data not shown). These results indicate that the PPARα is transported into the nuclei after translation, regardless of the absence or presence of added peroxisome proliferators, and that the intrinsic transactivation difference between the wild-type mPPARα and mPPARα-G cannot

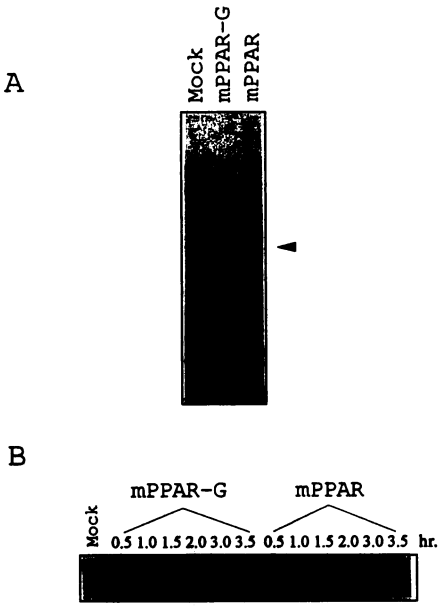

Fig. 3. Protein expression and stability comparisons between mPPARα and mPPARα-G from transfected COS-1 cells. Cells were transfected with pCMV-mPPARα (*mPPAR*), pCMV-mPPARα-G (*mPPAR-G*), or pCMV (*Mock*) with a DEAE-dextran method. After 72 hr, the cells were processed for immunoblotting or pulse labeling with Tran^{35}S-label as described in Materials and Methods. A, Immunoblot of the whole-cell lysates from COS-1 cells 72 hr after transfection. ^{125}I-Protein A was used to detect sequestered antibody. *Arrow*, Protein band with the expected mobility of the PPARα. B, Immunoprecipitation of whole-cell lysates from COS-1 cells transfected with either mPPARα or mPPARα-G and pulse labeled with Tran^{35}S-label for 1 hr. The cells were then chased with cold complete medium for the indicated times. Immunoprecipitated samples were separated with SDS-PAGE. Gel was treated with ENHANCE (DuPont), dried, and exposed to X-ray film.

be attributed to a difference in subcellular localization subsequent to protein synthesis.

DNA binding. Gel mobility shift assays were used to determine whether the COS-1 expressed mPPARs are equally competent to bind DNA *in vitro*. The PPARs displayed no apparent mobility difference when complexed with the Z element, which is a distal PPRE found in the upstream region of the *CYP4A6* gene (22), when whole-cell extracts from COS cells transfected with either mPPARα or mPPARα-G expression vectors were used as the source of receptor protein (Fig. 5). In addition, the presence or absence of a peroxisome proliferator (Wy-14,643) in the culture medium did not affect the mobility of the complex formed. When the antibody against mPPARα was added into the reaction mixture, a supershifted protein-DNA complex is detected. The complexes supershifted by the antibody exhibit slower mobilities which are similar for the two receptors, and the percentage of the complex shifted by the antibody is equal for the two PPARs (~50%) (Fig. 5). When PPARα-G is expressed in the absence of added Wy-14,643, there is no intrinsic activation in transfection experiments, yet this receptor binds the PPRE in EMSA experiments equally as well as the wild-type PPARα. In the presence of added Wy-14,643, PPARα-G effects a 5–10-fold increase in transcription but displays only a 10–20% increase in DNA binding. Clearly, the increased activation resulting from added Wy-14,643 and the difference in intrinsic activation cannot be explained by differences in the ability to bind DNA *in vitro*.

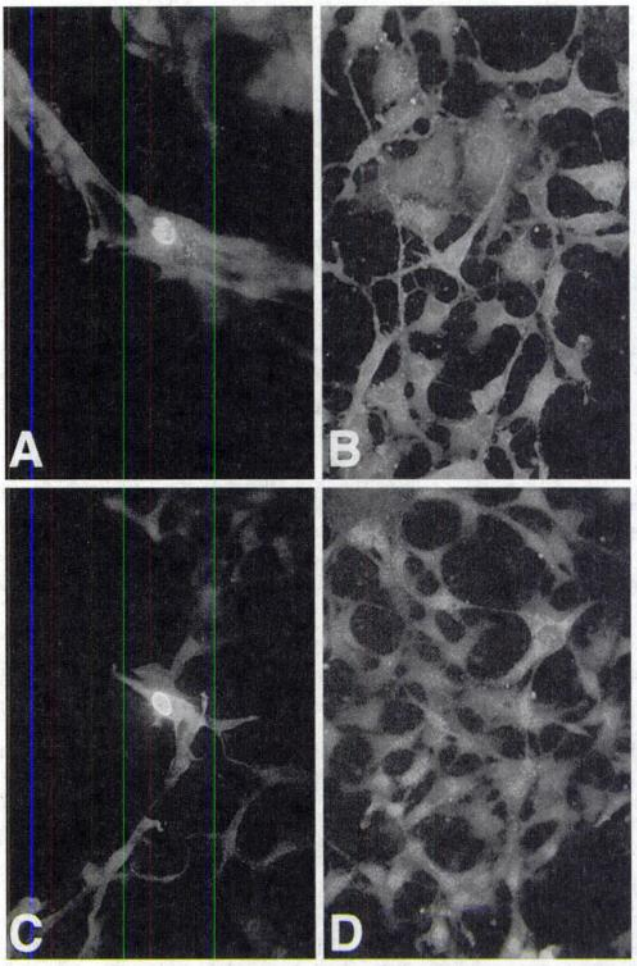

Fig. 4. Subcellular localization of mPPARα and mPPARα-G in transfected COS-1 cells. COS-1 cells were cultured in eight-well Lab-Tek chamber slides and transfected with pCMV-mPPARα, pCMV-mPPARα-G, or pCMV alone with a calcium phosphate method. The cells were treated with 50 μM Wy-14,643 or DMSO for 46 hr. After the media was removed, the cells were fixed with 4% paraformaldehyde. The slides were developed with rabbit anti-PPARα serum or preimmune serum and goat anti-rabbit IgG conjugated with fluorescein as described in Materials and Methods. The slides were analyzed with a Zeiss MC100 microscope (400× magnification). A, Cells transfected with pCMV-PPARα and treated with rabbit anti-PPARα serum. B, Cells transfected with pCMV-PPARα and treated with preimmune serum. C, Cells transfected with pCMV-PPARα-G and treated with anti-PPARα serum. D, Cells transfected with pCMV without insert and treated with anti-PPARα serum.

Overexpression of hRXRα with mPPARα. RXRα has been shown to facilitate the binding of mPPARα to PPREs found in the 5′ flanking regions of genes encoding P-450 4A6 (26), ACO (28), and the bifunctional enzyme (20). Experiments were conducted to examine whether overexpression of hRXRα would alter the phenotypic difference between mPPARα and mPPARα-G. Previous work in our laboratory (26) indicated that an additional PPRE adjacent to the transcription start site of *CYP4A6* could be unmasked by cotransfecting the mPPARα and hRXRα expression plasmids. For this reason, only the simpler ACO-TK reporter construct, which contains the A and B elements identified in the ACO gene (17), was used for these experiments. Cotransfection of hRXRα with either mPPARα or mPPARα-G did not affect the degree of intrinsic transactivation for mPPARα or mPPARα-G in either HepG2 or COS-1 cells (Fig. 6), regardless of

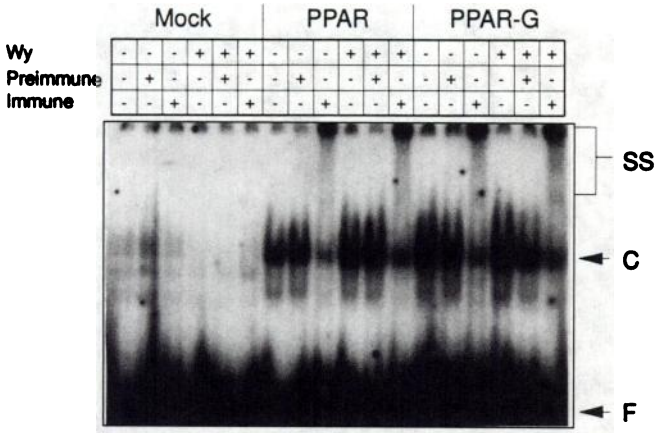

Fig. 5. PPARα and PPARα-G exhibit similar DNA binding *in vitro*. COS-1 cells were transfected with pSV-β-Gal and pCMV-mPPARα, pCMV-mPPARα-G, or pCMV with a DEAE-dextran method. At 24 hr after transfection, either 50 μM Wy-14,643 (+) or DMSO (−) was included in the culture medium for 48 hr. Cell lysates were prepared as described in Materials and Methods. Lysates (10–16 μg total protein) containing an equal amount of β-galactosidase activity were analyzed by EMSA for binding to ^{32}P-labeled double-stranded oligonucleotides corresponding to the *Z*-element (PPRE) of the *CYP4A6* gene (22). Protein-DNA complexes are seen in lanes with lysates containing either PPARα or PPARα-G (*C*) but not when lysates from COS cells transfected with the vector alone are used (*Mock*). Location of free oligonucleotide probe is indicated (*F*). Inclusion of rabbit anti-PPARα serum (*Immune*) in the binding assay resulted in the formation of lower mobility complexes (*SS*), of which a large proportion was retained at the origin. Addition of preimmune serum (*Preimmune*) did not result in shifted complexes.

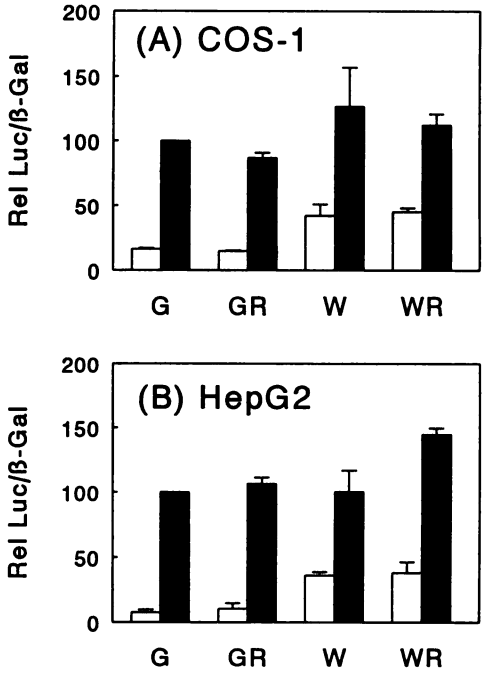

Fig. 6. Coexpression of hRXRα with mPPARα or mPPARα-G in COS-1 cells (A) and HepG2 cells (B); 1 μg pRS-hRXRα (*R*) or pRS was co-transfected with 50 ng pCMV-mPPARα (*W*) or pCMV-mPPARα-G (*G*). pLuc-TK-ACO was used as the reporter construct, and pSV-β-Gal plasmid served as the internal control. Cells were treated with 50 μM Wy-14,643 (*filled bar*) or DMSO (*open bar*) for 46 hr as described in Materials and Methods. Data are expressed as described for Fig. 1. Inclusion of 1 μM all-*trans*-retinoic acid did not change the results (data not shown).

the absence or presence of all-*trans*-retinoic acid. In addition, EMSA experiments with *E. coli* expressed affinity purified GST-PPARα and maltose binding protein-RXRα fusion proteins could not detect obvious differences between mPPARα and mPPARα-G with regard to an altered interaction with RXRα that might impair the ability of heterodimers to bind DNA (data not shown).

mPPARα-G exhibits a higher EC_{50} than the wild-type PPARα. When the dose-response curves of pLuc-4A6–880 in the presence of either mPPARα or mPPARα-G were compared, a ~4-fold higher EC_{50} value for Wy-14,643 was observed for the mPPARα-G receptor relative to the wild-type receptor in HepG2 cells (Fig. 7, *triangles*). The level of transactivation by Wy-14,643 is saturable with both forms of mPPARα, and the maximum levels obtained are similar. When pLuc-TK-ACO was used as the reporter, a 5-fold higher EC_{50} value also was found for the mPPARα-G when compared with the wild-type for Wy-14,643 in HepG2 cells (Fig. 7, *circles*) and RK_{13} cells (data not shown). The level of transactivation effected by Wy-14,643 was also saturable with both forms of PPARα, and the maximum levels obtained were similar. For each receptor, the EC_{50} values determined for pLuc-TK-ACO were ~3-fold higher than those obtained with the pLuc-4A6–880 reporter.

A structurally distinct activator, ETYA, which is a synthetic analogue of arachidonic acid bearing triple rather than double unsaturated bonds, was also tested. For the pLuc-4A6–880 reporter, the difference in EC_{50} in the presence of ETYA between mPPARα and mPPARα-G is similar to that observed for Wy-14,643 (Fig. 8A). ETYA was reported to be more potent than Wy-14,643 for *Xenopus* PPARα (28); however, it is 10-fold less potent than Wy-14,643 for the murine PPARα. Although the EC_{50} value for ETYA is higher than that observed for Wy-14,643, the maximum level of transactivation effected by ETYA was found to be equal to the maximum response produced by Wy-14,643. Similar results were obtained in RK_{13} cells (data not shown). For the pLuc-TK-ACO reporter, a higher EC_{50} value was also seen with mPPARα-G than the wild-type receptor. In addition, the dose-response curves had a cooperative appearance (Fig. 8B). The data could not be fitted with the one-site ligand model, and a sigmoidal equation was used. There was no apparent response for the pLuc-TK-ACO at low doses where a response was detected for the pLuc-4A6–880 reporter. This apparent threshold seen for pLuc-TK-ACO is therefore unlikely to reflect poor ETYA availability, cellular uptake, or both. Nevertheless, the EC_{50} values for ETYA obtained with pLuc-TK-ACO for both receptors were higher than the values obtained with the pLuc-4A6–880 reporter, as was seen with Wy-14,643.

Role of fatty acids in PPARα-mediated gene transactivation. Fatty acids have been proposed to be endogenous ligands for PPAR (15) and have been shown to activate PPAR-mediated transcription (28, 36, 37) in gene transfer experiments. Palmitic acid, an abundant endogenous saturated fatty acid, was previously shown to activate mPPARα (38). Therefore, palmitic acid was added to the cell culture medium to see if the phenotypic difference between the mPPARs that is evident with Wy-14,643 and ETYA also exists for these potential endogenous activator. Due to the lack of a response in HepG2 cells to the addition of palmitic acid, RK_{13} cells were used for all subsequent experiments. Also, the

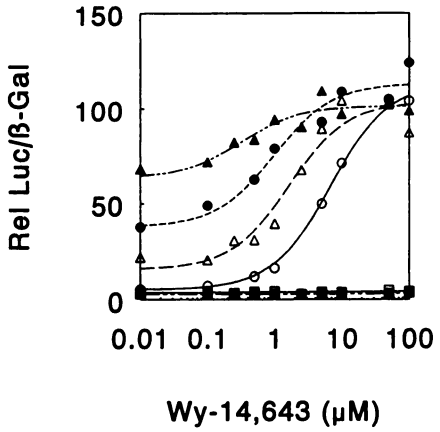

Fig. 7. Dose-response curves of the transactivation of pLuc-4A6–880 or pLuc-TK-ACO by Wy-14,643 in the presence of mPPARα or mPPARα-G in HepG2 cells. pCMV-mPPARα (*filled symbols*), pCMV-mPPARα-G (*open symbols*), or pCMV (*squares*) was transfected with reporter constructs pLuc-4A6–880 (*triangles*) or pLuc-TK-ACO (*circles*) into cells as described in Materials and Methods. The pSV-βGal plasmid was included in the transfection as an internal control. Data are expressed relative to the normalized luciferase activity obtained from cells transfected with mPPARα-G and treated with 50 μM Wy-14,643. This value was arbitrarily set to 100. The final concentration of Wy-14,643 added to the medium is indicated on the *x*-axis. Each data point is the average of at least three transfections. For each transfection, triplicate determinations were obtained for each experimental condition. Nonlinear regression was used to generate the curves shown and to estimate the EC_{50} values using the one-site ligand-binding equation described in Materials and Methods. The calculated EC_{50} values and their standard errors (μM) were, for pLuc-4A6–880, mPPARα, 0.3 ± 0.1; mPPARα-G, 1.6 ± 0.6; for pLuc-TK-ACO, mPPARα, 1.0 ± 0.3; mPPARα-G, 7.0 ± 0.6.

pLuc-TK-ACO reporter was used because of the high level of intrinsic transactivation of the pLuc-4A6–880 reporter with the wild-type mPPARα in RK_{13} cells.

When palmitic acid was used to determine the dose-response curves for both mPPARs, a saturable response was seen with the mPPARα but not with mPPARα-G (Fig. 9). A higher concentration of palmitic acid could not be used due to limited solubility and noticeably altered cellular morphology. Palmitic acid also activated pLuc-TK-ACO to a small extent (15% of the maximum response seen with Wy-14,643) at the highest concentrations tested without cotransfected mPPARα or mPPARα-G (data not shown). When the pLuc-4A6–880 reporter was used, mPPARα-G also could not effect a saturable transactivation in the presence of 100 μM palmitic acid in RK_{13} cells (data not shown). Obviously, the concentration of palmitic acid required to elicit full activation is much higher than that required for Wy-14,643 or ETYA. This could reflect poor cellular uptake, efficient cellular metabolism, or both, which could limit the amount of palmitic acid available for receptor activation. The latter is suggested by the inability of palmitic acid to activate either reporter construct in HepG2 cells in the presence of either mPPARα (data not shown) as HepG2 cells have been shown to efficiently metabolize fatty acids (39). Therefore, these results may not reflect the concentrations available for activation because the impact of cellular uptake and disposition on intracellular concentration is unknown. Although the EC_{50} values for the two receptors cannot be directly compared due to a lack of saturation seen with mPPARα-G, the saturable response seen with the wild-type receptor suggests that the lower EC_{50} value with mPPARα for Wy-14,643 or ETYA, compared with mPPARα-G, may also exist for putative endogenous activators, such as palmitic acid.

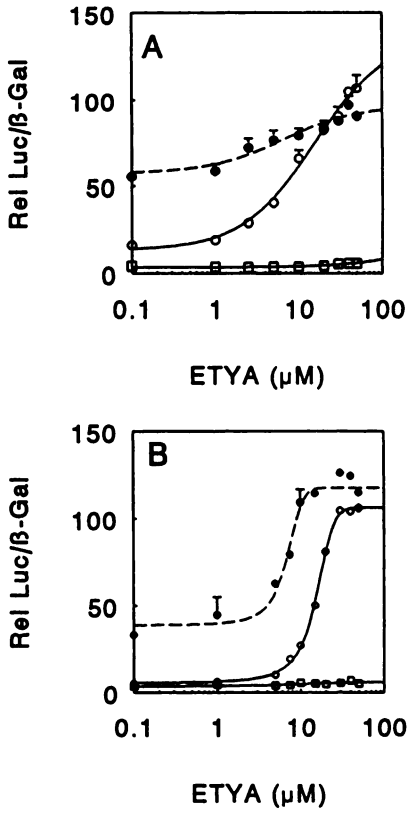

Fig. 8. Dose-response curves of the transactivation of pLuc-4A6–880 (A) or pLuc-TK-ACO (B) by ETYA in the presence of either mPPARα or mPPARα-G in HepG2 cells. pCMV-mPPARα (●), pCMV-mPPARα-G (○), or pCMV (□) was transfected with the pLuc-TK-ACO reporter construct into cells as described in Materials and Methods. pSV-βGal plasmid was included in the transfection as an internal control. Data are expressed as described for Fig. 7. Nonlinear regression was used to generate the curves shown and to estimate the EC_{50} values. A, A one-site ligand-binding equation was used for curve-fitting; B, a sigmoidal equation was used for curve-fitting, as described in Materials and Methods. The calculated EC_{50} values and their standard errors (μM) were: for pLuc-4A6–880: mPPARα, 3.4 ± 1.3; mPPARα-G, 10.9 ± 3.0; for pLuc-TK-ACO: mPPARα, 6.7 ± 0.6; mPPARα-G, 15.4 ± 0.3.

Discussion

Previous studies in our laboratory (22) demonstrated transactivation of a *CYP4A6* reporter construct by mPPARα in three different cell lines in the absence of added peroxisome proliferators (intrinsic transactivation). This transactivation by PPARα has been noted for other genes (2, 3, 27, 29, 30), but it is more pronounced for the *CYP4A6* reporter construct and accounts for as much as 80% of the transactivation seen in the presence of added peroxisome activators. A mutant, mPPARα-G, which carries a glycine at amino acid position 282 instead of glutamic acid (22), exhibits a very low intrinsic transactivation but fully activates transcription in the presence of peroxisome proliferators. As shown by the present study, the wild-type and mutant PPARs exhibit similar levels of protein expression and turnover. Both transiently expressed receptors are localized in the nucleus and bind equally *in vitro* to the *CYP4A6* PPRE (Z element) in the

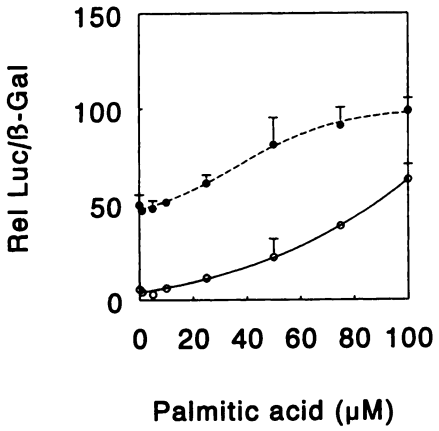

Fig. 9. Dose-response curves of the transactivation of pLuc-TK-ACO by mPPARα or mPPARα-G in the presence of palmitic acid. pCMV-mPPARα, pCMV-mPPARα-G, or pCMV was transfected into RK_{13} cells with the pLuc-TK-ACO reporter construct as described in Materials and Methods. Data are expressed as described for Fig. 1. Normalized data for PPARα (●) and PPARα-G (○) were then corrected by subtracting the normalized data obtained with pCMV alone (data not shown), which exhibited a value of 5 for 0–75 μM palmitic acid and increased to 19.7 for 100 μM palmitic acid. Curves were generated by nonlinear regression with the use of a sigmoidal equation.

presence or absence of added Wy-14,643. The mutant mPPARα-G was found to exhibit a higher EC_{50} value with the potent peroxisome proliferators Wy-14,643 and ETYA with each reporter in each cell line. The dose-response curves of pLuc-TK-ACO to added palmitic acid (Fig. 9) suggest that the higher EC_{50} values displayed by the mutant mPPARα-G may also exist for palmitic acid and other fatty acids, which have been suggested to be endogenous activators for PPARα (15).

A higher intrinsic transactivation and a lower EC_{50} value for ETYA and Wy-14,643 were seen consistently with the wild-type receptor compared with mPPARα-G, although the level of intrinsic transactivation and the EC_{50} values were found to differ between the two reporter constructs. In general, the degree of intrinsic activation was inversely related to the EC_{50} values observed for exogenous peroxisome proliferators. This suggests that the intrinsic transactivation may reflect the presence of an endogenous activator at a concentration that can significantly transactivate the wild-type mPPARα but not the mPPARα-G due to the higher apparent EC_{50} value for the latter. Differences in intrinsic transactivation have also been reported among the different forms of *X. laevis* PPAR: α, β, and γ (3, 37). xPPARβ and xPPARγ exhibit higher EC_{50} values for ETYA when compared with xPPARα (37), and they also show lower intrinsic transactivation of TK-ACO than xPPARα (3, 37).

An inverse correlation between the intrinsic transactivation and the EC_{50} value was also seen between reporter constructs in the present study (Fig. 7). The lower intrinsic transactivation seen with the pLuc-TK-ACO construct compared with the pLuc-4A6–880 construct in the three studied cell lines may reflect the higher apparent EC_{50} values determined for pLuc-TK-ACO with ETYA and Wy-14,643 than for pLuc-4A6–880. Comparison of the dose-response curves obtained with either pLuc-4A6–880 or pLuc-TK-ACO clearly indicates that the EC_{50} values obtained with Wy-14,643 and ETYA for both receptors with pLuc-4A6–880 are 2–3-fold lower than the values seen with pLuc-TK-ACO in HepG2 cells. Although the exact mechanism for this difference is unclear, it may be due to differences in the identities of other transcription factors that interact with PPARα during the transcriptional activation of the two reporter constructs. The pLuc-4A6–880 construct not only contains multiple PPREs (X, Z, and -27) but also contains the natural promoter for the 4A6 gene (22, 26). The pLuc-TK-ACO construct is a relatively simple construct that contains only one PPRE linked to a heterologous promoter. However, there are, in addition to the PPRE, other sequences from the ACO gene (B element) included in the pLuc-TK-ACO reporter construct (17) that have been reported to enhance the response of the ACO PPRE without binding to PPARα directly.

The sigmoidal nature of the ETYA dose-response curves with pLuc-TK-ACO for both receptors suggests the possibility of cooperative behavior. This behavior was not seen with pLuc-TK-ACO plus Wy-14,643 or with pLuc-4A6–880 plus Wy-14,643 or ETYA in HepG2 cells. It is interesting to note that ETYA activates transcription at high concentrations in the absence of the heterologous expression of either PPARα in RK_{13} cells (data not shown). The mechanism of this activation has not been extensively investigated, but it is possible that it acts cooperatively with the ETYA stimulation of PPARα. This cooperative behavior may be obscured for the pLuc-4A6–880 reporter because of the multiplicity of PPARα response elements found in this reporter construct. The underlying mechanism for the cooperative behavior is unclear and will require further investigation.

In summary, a higher intrinsic transactivation and a lower EC_{50} value were consistently seen with mPPARα compared with mPPARα-G with each reporter construct. A high affinity ligand, thiazolidinedione, has been shown to bind PPARγ directly (40), suggesting that PPARα may also be activated by a bound ligand. The higher EC_{50} value seen with the mPPARα-G could indicate that the amino acid change alters the ability of the receptor to bind activators or antagonists. The EC_{50} difference may also result from an altered interaction with other transcriptional factors that interact with PPARα in DNA binding and transactivation. Thus, the mutation might affect the efficacy of PPARα-mediated transactivation rather than receptor occupancy by putative ligands. Investigation of the affects associated with the G mutation should help to understand various receptor parameters (e.g., ligand-binding site, ligand dissociation constant, receptor occupancy, and receptor efficacy), that contribute to the transcription of responsive genes and allow a clearer understanding of the signal transduction pathways by which peroxisome proliferators mediate gene regulation.

Acknowledgments

We express our appreciation to Drs. D. J. Manglesdorf and R. Evans (Salk Institute, La Jolla, CA) for providing the hRXRα cDNA in the pRSV expression plasmid. The authors acknowledge Y. Wang and R. Casey for their technical assistance.

References

1. Issemann, I., and S. Green. Activation of a member of the steroid hormone receptor superfamily by peroxisome proliferators. *Nature (Lond.)* **347**:645–650 (1990).
2. Sher, T., H.-F. Yi, O. W. McBride, and F. J. Gonzalez. cDNA cloning, chromosomal mapping, and functional characterization of the human peroxisome proliferator activated receptor. *Biochemistry* **32**:5598–5604 (1993).
3. Dreyer, C., G. Krey, H. Keller, F. Givel, G. Helftenbein, and W. Wahli. Control of the peroxisomal β-oxidation pathway by a novel family of nuclear hormone receptors. *Cell* **68**:879–887 (1992).

4. Göttlicher, M., E. Widmark, Q. Li, and J.-Å. Gustafsson. Fatty acids activate a chimera of the clofibric acid-activated receptor and the glucocorticoid receptor. *Proc. Natl. Acad. Sci. USA* **89:**4653–4657 (1992).
5. Green, S. Receptor-mediated mechanisms of peroxisome proliferators. *Biochem. Pharmacol.* **43:**393–401 (1992).
6. Nilsson, R., B. Beije, V. Préat, K. Erixon, and C. Ramel. On the mechanism of the hepatocarcinogenicity of peroxisome proliferators. *Chem. Biol. Interact.* **78:**235–250 (1991).
7. Rao, M. S., and J. K. Reddy. An overview of peroxisome proliferator-induced hepatocarcinogenesis. *Environ. Health Perspect.* **93:**205–209 (1991).
8. Bentley, P., I. Calder, C. Elcombe, P. Grasso, D. Stringer, and H.-J. Wiegand. Hepatic peroxisome proliferation in rodents and its significance for humans. *Food Chem. Toxicol.* **31:**857–907 (1993).
9. Bell, D. R., and C. R. Elcombe. Induction of acyl-CoA oxidase and cytochrome P450IVA1 RNA in rat primary hepatocyte culture by peroxisome proliferators. *Biochem. J.* **280:**249–253 (1991).
10. Bars, R. G., D. R. Bell, and C. R. Elcombe. Induction of cytochrome P450 and peroxisomal enzymes by clofibric acid *in vivo* and *in vitro*. *Biochem. Pharmacol.* **45:**2045–2053 (1993).
11. Bell, D. R., R. G. Bars, G. G. Gibson, and C. R. Elcombe. Localization and differential induction of cytochrome P450IVA and acyl-CoA oxidase in rat liver. *Biochem. J.* **275:**247–252 (1991).
12. Muerhoff, A. S., K. J. Griffin, and E. F. Johnson. Characterization of a rabbit gene encoding a clofibrate-inducible fatty acid ω-hydroxylase: *CYP4A6*. *Arch. Biochem. Biophys.* **296:**66–72 (1992).
13. Banner, C. D., M. Göttlicher, E. Widmark, J. Sjövall, J. J. Rafter, and J.-Å. Gustafsson. A systematic analytical chemistry/cell assay approach to isolate activators of orphan nuclear receptors from biological extracts: characterization of peroxisome proliferator-activated receptor activators in plasma. *J. Lipid Res.* **34:**1583–1591 (1993).
14. Issemann, I., R. Prince, J. Tugwood, and S. Green. A role for fatty acids and liver fatty acid binding protein in peroxisome proliferation. *Biochem. Soc. Trans.* **20:**824–827 (1992).
15. Keller, H., and W. Wahli. Peroxisome proliferator-activated receptors: a link between endocrinology and nutrition. *Trends Endocrinol. Metab.* **4:**291–296 (1993).
16. Green, S., and W. Wahli. Peroxisome proliferator-activated receptors: finding the orphan a home. *Mol. Cell. Endocrinol.* **100:**149–153 (1994).
17. Osumi, T., J.-K. Wen, and T. Hashimoto. Two *cis*-acting regulatory sequences in the peroxisome proliferator-responsive enhancer region of rat acyl-CoA oxidase gene. *Biochem. Biophys. Res. Commun.* **175:**866–871 (1991).
18. Tugwood, J. D., I. Issemann, R. G. Anderson, K. R. Bundell, W. L. McPheat, and S. Green. The mouse peroxisome proliferator activated receptor recognizes a response element in the 5′ flanking sequence of the rat acyl CoA oxidase gene. *EMBO J.* **11:**433–439 (1992).
19. Zhang, B., S. L. Marcus, F. G. Sajjadi, K. Alvares, J. K. Reddy, S. Subramani, R. A. Rachubinski, and J. P. Capone. Identification of a peroxisome proliferator-responsive element upstream of the gene encoding rat peroxisomal enoyl-CoA hydratase/3-hydroxyacyl-CoA dehydrogenase. *Proc. Natl. Acad. Sci. USA* **89:**7541–7545 (1992).
20. Bardot, O., T. C. Aldridge, N. Latruffe, and S. Green. PPAR-RXR heterodimer activates a peroxisome proliferator response element upstream of the bifunctional enzyme gene. *Biochem. Biophys. Res. Commun.* **192:**37–45 (1993).
21. Aldridge, T. C., J. D. Tugwood, and S. Green. Identification and characterization of DNA elements implicated in the regulation of CYP4A1 transcription. *Biochem. J.* **306:**473–479 (1995).
22. Muerhoff, A. S., K. J. Griffin, and E. F. Johnson. The peroxisome proliferator activated receptor mediates the induction of *CYP4A6*, a cytochrome P450 fatty acid ω-hydroxylase, by clofibric acid. *J. Biol. Chem.* **267:**19051–19053 (1992).
23. Kliewer, S. A., K. Umesono, D. J. Noonan, R. A. Heyman, and R. M. Evans. Convergence of 9-*cis* retinoic acid and peroxisome proliferator signalling pathways through heterodimer formation of their receptors. *Nature (Lond.)* **358:**771–774 (1992).
24. Miyata, K. S., B. Zhang, S. L. Marcus, J. P. Capone, and R. A. Rachubinski. Chicken ovalbumin upstream promoter transcription factor (COUP-TF) binds to a peroxisome proliferator-responsive element and antagonizes peroxisome proliferator-mediated signaling. *J. Biol. Chem.* **268:**19169–19172 (1993).
25. Gearing, K. L., M. Göttlicher, M. Teboul, E. Widmark, and J.-Å. Gustafsson. Interaction of the peroxisome-proliferator-activated receptor and retinoid X receptor. *Proc. Natl. Acad. Sci. USA* **90:**1440–1444 (1993).
26. Palmer, C. N. A., M.-H. Hsu, A. S. Muerhoff, K. J. Griffin, and E. F. Johnson. Interaction of the peroxisome proliferator-activated receptor α with the retinoid X receptor α unmasks a cryptic peroxisome proliferator response element that overlaps an ARP-1-binding site in the *CYP4A6* promoter. *J. Biol. Chem.* **269:**18083–18089 (1994).
27. Marcus, S. L., K. S. Miyata, B. Zhang, S. Subramani, R. A. Rachubinski, and J. P. Capone. Diverse peroxisome proliferator-activated receptors bind to the peroxisome proliferator-responsive elements of the rat hydratase/dehydrogenase and fatty acyl-CoA oxidase genes but differentially induce expression. *Proc. Natl. Acad. Sci. USA* **90:**5723–5727 (1993).
28. Keller, H., C. Dreyer, J. Medin, A. Mahfoudi, K. Ozato, and W. Wahli. Fatty acids and retinoids control lipid metabolism through activation of peroxisome proliferator-activated receptor-retinoid X receptor heterodimers. *Proc. Natl. Acad. Sci. USA* **90:**2160–2164 (1993).
29. Zhu, Y., K. Alvares, Q. Huang, M. S. Rao, and J. K. Reddy. Cloning of a new member of the peroxisome proliferator-activated receptor gene family from mouse liver. *J. Biol. Chem.* **268:**26817–26820 (1993).
30. Rodríguez, J. C., G. Gil-Gómez, F. G. Hegardt, and D. Haro. Peroxisome proliferator-activated receptor mediates induction of the mitochondrial 3-hydroxy-3-methylglutaryl-CoA synthase gene by fatty acids. *J. Biol. Chem.* **269:**18767–18772 (1994).
31. Cullen, B. R. Use of eukaryotic expression technology in the functional analysis of cloned genes. *Methods Enzymol.* **152:**684–704 (1987).
32. Towbin, H., S. Theophil, and J. Gordon. Electrophoretic transfer of proteins from polyacrylamide gels to nitrocellulose sheets: procedure and some applications. *Proc. Natl. Acad. Sci. USA* **76:**4350–4354 (1979).
33. Sambrook, J., E. F. Fritsch, and T. Maniatis. *Molecular Cloning: A Laboratory Manual*. Cold Spring Harbor Laboratory Press, Cold Spring Harbor, NY (1989).
34. Dreyer, C., H. Keller, A. Mahfoudi, V. Laudet, G. Krey, and W. Wahli. Positive regulation of the peroxisomal β-oxidation pathway by fatty acids through activation of peroxisome proliferator-activated receptors (PPAR). *Biol. Cell* **77:**67–76 (1993).
35. Kainu, T., A.-C. Wikström, J.-Å. Gustafsson, and M. Pelto-Huikko. Localization of the peroxisome proliferator-activated receptor in the brain. *Neuroreport* **5:**2481–2485 (1994).
36. Göttlicher, M., A. Demoz, D. Svensson, P. Tollet, R. K. Berge, and J.-Å. Gustafsson. Structural and metabolic requirements for activators of the peroxisome proliferator-activated receptor. *Biochem. Pharmacol.* **46:**2177–2184 (1993).
37. Krey, G., H. Keller, A. Mahfoudi, J. Medin, K. Ozato, C. Dreyer, and W. Wahli. *Xenopus* peroxisome proliferator activated receptors: genomic organization, response element recognition, heterodimer formation with retinoid X receptor and activation by fatty acids. *J. Steroid Biochem. Mol. Biol.* **47:**65–73 (1993).
38. Issemann, I., R. A. Prince, J. D. Tugwood, and S. Green. The peroxisome proliferator-activated receptor:retinoid X receptor heterodimer is activated by fatty acids and fibrate hypolipidaemic drugs. *J. Mol. Endocrinol.* **11:**37–47 (1993).
39. Watkins, P. A., E. V. Ferrell, Jr., J. I. Pedersen, and G. Hoefler. Peroxisomal fatty acid β-oxidation in HepG2 cells. *Arch. Biochem. Biophys.* **289:**329–336 (1991).
40. Lehmann, J. M., L. B. Moore, T. A. Smith-Oliver, W. O. Wilkison, T. M. Willson, and S. A. Kliewer. An antidiabetic thiazolidinedione is a high affinity ligand for peroxisome proliferator-activated receptor γ (PPARγ). *J. Biol. Chem.* **270:**12953–12956 (1995).
41. Nelson, D. R., T. Kamataki, D. J. Waxman, F. P. Guengerich, R. W. Estabrook, R. Feyereisen, F. J. Gonzalez, M. J. Coon, I. C. Gunsalus, O. Gotoh, K. Okuda, and D. W. Nebert. The P450 superfamily: update on new sequences, gene mapping, accession numbers, early trivial names of enzymes, and nomenclature. *DNA Cell Biol.* **12:**1–51 (1993).

Send reprint requests to: Eric F. Johnson, Ph.D., Division of Biochemistry, NX-4, The Scripps Research Institute, 10666 N. Torrey Pines Road, La Jolla, CA 92037.